Myopia

13

Ichiro Maruko and Tomohiro Iida

13.1 Introduction

Myopia is functionally classified into two groups: non-pathologic myopia and pathologic myopia. Non-pathologic myopia is usually a minimal to moderate degree of myopia (usually less than 6 diopters), and includes simple myopia or "school myopia." Non-pathologic myopia has no disorder other than reflective error and is easy to correct with glasses. Although there is no international standard definition, pathologic myopia is generally defined as either a reflective error of more than 8 diopters or an axial length of more than 26.5 mm. Pathologic myopia often causes a variety of fundus changes called myopic maculopathy, choroidal neovascularization (CNV), myopic retinoschisis, foveal retinal detachment, or macular hole [1].

The static visual field test is thought to be unsuitable to evaluate the abnormality in patients with pathologic myopia because these patients often have myopic maculopathy or a large peripapillary conus. Recently, new technology has produced the Microperimeter-1 (MP-1, NIDEK, Italy), as a detailed functional examination device. This chapter describes the abnormal visual field in pathologic myopia using MP-1.

I. Maruko, MD (✉) • T. Iida
Department of Ophthalmology,
Tokyo Women's Medical University
School of Medicine, 8-1 Kawada-cho,
Shinjuku-ku, Tokyo, Japan
e-mail: imaruko@oph.twmu.ac.jp

13.2 Ophthalmoscopic Findings

As known, the fundus in pathologic myopia shows various changes. Tigroid fundus is the most common myopic sign even in simple myopia. It is thought to result from the thinning of retinal pigment epithelium (RPE) associated with elongation of the axial length. Myopic conus, which is induced by dissociation between the optic disc and its surrounding tissue, is also common. Focal and/or diffuse atrophic lesions are observed in all types of high myopia and these lesions indicate RPE degeneration, which is caused by a decreased blood supply from the choriocapillaris. These lesions can appear as brown or white areas resulting from the pigmentation or depigmentation of RPE. Lacquer crack lesions are the mechanical breaking of the Bruch's membrane. It is difficult to determine their length and width on ophthalmoscopic observation. At fundus autofluorescence, they appear as noninvasive hypofluorescent lines. Generally, posterior staphyloma develops after age 40 in severe myopia. The reason for the formation of posterior staphyloma has not yet been identified. The extent of staphyloma can be visualized using magnetic resonance imaging (MRI) according to recent reports [2, 3]. CNV appears on ophthalmoscopic examination as a gray lesion at the fovea and it is sometimes accompanied by subretinal hemorrhage. On fluorescent angiography, CNV is observed as the classic type with hyperfluorescence at the beginning of the early

E. Midena (ed.), *Microperimetry and Multimodal Retinal Imaging*,
DOI 10.1007/978-3-642-40300-2_13, © Springer-Verlag Berlin Heidelberg 2014

phase and late leakage. Old CNV lesions remain as pigmented findings at the fovea, which are also called "Fuchs' spots".

13.3 Optical Coherence Tomography Findings

Optical coherence tomography (OCT) is the most valuable device for the imaging of the macular area. In pathologic myopia, OCT can visualize detailed morphologic changes that cannot be observed in a routine ophthalmic examination [4, 5]. It is very suitable to observe a foveal retinal detachment using OCT because of minimal changes. Myopic foveal retinal detachment is frequently accompanied by foveal retinoschisis. Foveal retinoschisis is one of the visual loss causes in pathologic myopia and it has recently been considered a major contributor of foveal retinal detachment and macular holes [6–8]. Foveal morphologic impairment in pathologic myopia is classified into three groups: the retinoschis type, the foveal detachment type and the macular hole type. This classification is essential for the prediction of visual prognosis [9, 10]. It is easy to distinguish these types on the Spectral OCT domain. Recent micro-incision vitreous surgery, even for retinoschisis, is safe and effective as long as the formation of macular holes are avoided.

CNV is the main cause of central visual loss in pathologic myopia [11]. A typical case of myopic CNV is categorized as type 2 CNV, which extends into the subretinal space. Myopic CNV is generally observed as hyperreflective tissue above the RPE line.

Another type of foveal retinal detachment formation in pathologic myopia has recently been reported. Dome-shaped macula (DSM) is a new entity associated with highly myopic eyes [12]. It might be a particular type of posterior staphyloma, and defined as a convex elevation of the macula on OCT. Subretinal fluid is sometimes observed in DSM, and it may cause the choroidal outflow disorder associated with local morphological changes of choroid and sclera at the fovea [13]. Although the tilted disc syndrome is usually associated with good visual prognosis, foveal complications, such as foveal retinal detachment, are sometimes observed. Tilted disc syndrome is often accompanied by moderate to severe myopic refractive error. Foveal retinal detachment in tilted disc syndrome, together with DSM, is thought to be a local morphologic change associated with the inferior staphyloma [14].

13.4 Microperimetry for Pathologic Myopia

OCT can capture subtle morphologic changes, but cannot evaluate functional changes. Although visual acuity is still a traditional valuable indicator for visual function, it reflects only the status of fovea and perifovea. On the other hand, the perimeter reflects a much wider macular area function than visual acuity. MP-1 microperimeter is the recently developed device that can provide the automatic lesion-related perimetry for monitoring the fundus.

The characteristics of MP-1 are the auto eye-tracking system for involuntary eye movements, the follow-up mode, the possibility of creating composed images using color fundus photos and perimetry results and the possibility of customizing patterns of stimulus points. The auto tracking system is an advantage during the examination, especially in pathologic myopia. Composite images of a fundus photo and sensitivity results are useful for evaluating the various lesions of myopic maculopathy. However, the operator should pay attention to the overlay of fundus photos and perimetry results because of the blurry images in highly myopic eyes. CNV size in pathologic myopia might be smaller than in age-related macular degeneration. It is useful to evaluate the small changes correctly using the customized stimulus points in an MP-1. A follow-up mode is helpful for measuring small changes in small lesions. There are several reports about microperimetry in eyes with pathologic myopia [15–23]; several cases are discussed in more detail below.

13.5 Case Presentation

13.5.1 Dome-Shaped Macula (DSM) (Fig. 13.1)

DSM is a new pathologic myopia-related entity, which is sometimes associated with subretinal fluid. Gaucher et al. originally reported that it can be found in the 20 % of all highly myopic eyes [12]. We evaluate DSM using spectral domain OCT and the subretinal fluid due to the relative scleral thickening at the subfovea. There are no reports of using MP-1 for DSM.

Figure 13.1 refers to a case of a 71-years-old woman with bilateral blur vision. Decimal visual acuities with intraocular lenses in both eyes are 0.9 in the right eye and 0.7 in the left eye. Her axial lengths are 34.44 mm in the right eye and 34.06 mm in the left. Both eyes show a large peripapillary conus and widespread RPE atrophy. A swept source OCT captures the convex elevation of the macula in both eyes. Using MP-1, almost normal sensitivity is measured in the right eye and relatively low sensitivity in the left eye. These findings correlate with the higher macular elevation of the left eye compared to the right eye.

13.5.2 Tilted Disc Syndrome (TDS) (Fig. 13.2)

TDS is known as the characteristic inferonasal tilting of the optic disc, associated with congenital inferonasal crescent and inferior staphyloma. Staphyloma in TDS is often observed in the inferior ocular area, and the superior edge of the staphyloma sometimes involves the macula; this is the reason why these anatomic changes at the superior edge of the staphyloma may lead to foveal weakness and subsequent complications.

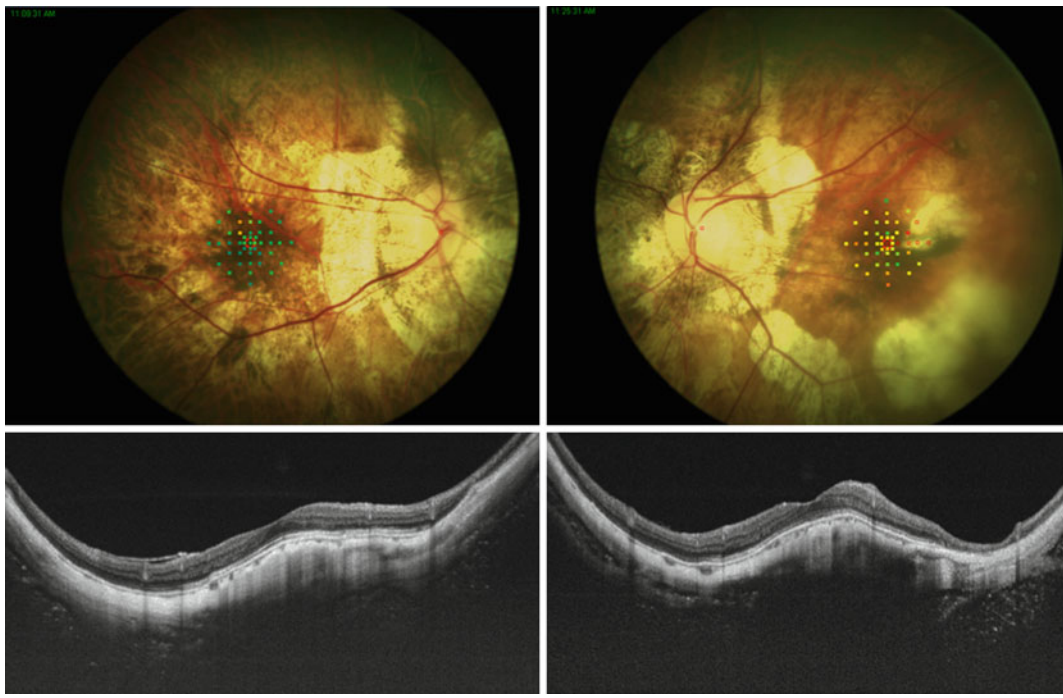

Fig. 13.1 Dome-shaped macula. A 71-year-old female. Best-collected visual acuity is 0.9 in the right eye and 0.7 in the left eye. Axial length is 34.44 mm in the right eye and 34.06 mm in the left eye (*top column*). Microperimetry-1 results with composite fundus photo in both eyes. Right eye is almost normal, however left eye shows the partial scotoma corresponding to the chorioretinal atrophy (*bottom column*). Vertical scan images of swept source optical coherence tomography in both eyes reveal the convex elevation of the macula. There is no subretinal fluid at all

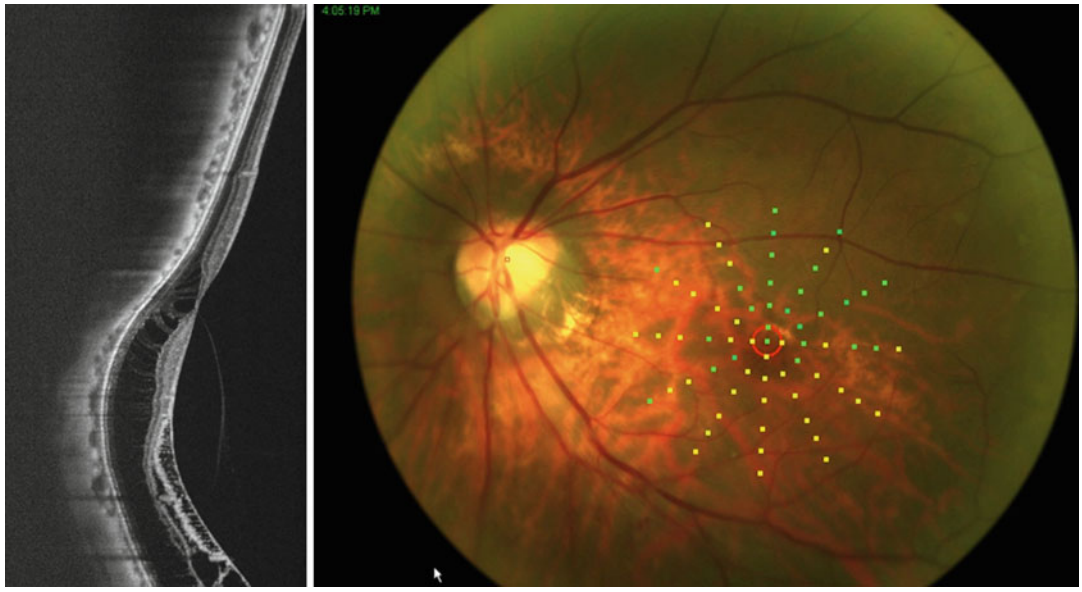

Fig. 13.2 Tilted disc syndrome. A 63-year-old female. Decimal visual acuity is 0.4 in the left eye. The spherical equivalent is −12 diopters and axial length is 27.09 mm in the left eye (*right*). Color fundus shows the inferior-nasal tilted disc with conus. Microperimetry-1 results show relative lower sensitivity at the inferior half than superior half of the macula (*left*). Vertical scan of swept source optical coherence tomography shows retinoschisis at the inferior macula

Figure 13.2 refers to a 63-year-old woman with 0.4 decimal visual acuity in the left eye. The spherical equivalent is −12 diopters and the axial length is 27.09 mm in the left eye. Inferior staphyloma is observed with retinoschisis on swept-source OCT. Relatively less sensitivity on MP-1 is measured in correspondence of the inferior staphyloma with retinoschisis.

13.5.3 Macular Hole Retinal Detachment (MHRD) (Fig. 13.3)

MHRD is one of the most serious complications in pathologic myopia; myopic CNV is the other complication associated with severe visual loss.

Figure 13.3 refers to a case of a 70-year-old woman with a history of CNV removal surgery. Axial length is 29.57, and decimal visual acuity is 0.5 in the right eye. Large RPE atrophy is observed at the macular area where a low sensitivity is also measured. One year later, MHRD appears at the macula, and MP-1 shows a further sensitivity decrease.

13.5.4 Myopic Choroidal Neovascularization (Myopic CNV) (Fig. 13.4)

Myopic CNV induces central visual loss and scotoma. Recently, bevacizumab, an anti-vascular endothelial growth factor, has been

Fig. 13.4 Myopic choroidal neovascularization. A 72-year-old female with myopic choroidal neovascularization in the right eye. Axial length on the right eye is 28.58 mm (*top left*). Fluorescein angiography at baseline shows the classic choroidal neovascularization lesion with leakage on the early phase (*top right*). Optical coherence tomography shows the hyperreflective tissue above retinal pigment epithelium representative characteristics of type 2 choroidal neovascularization lesion (*bottom left*). Microperimetry-1 results at the baseline shows the reduced sensitivity at the area of the choroidal neovascularization lesion (*bottom right*). One month after intravitreal bevacizumab, visual acuity did not change at all, but the slight improvement was measured on Microperimetry-1

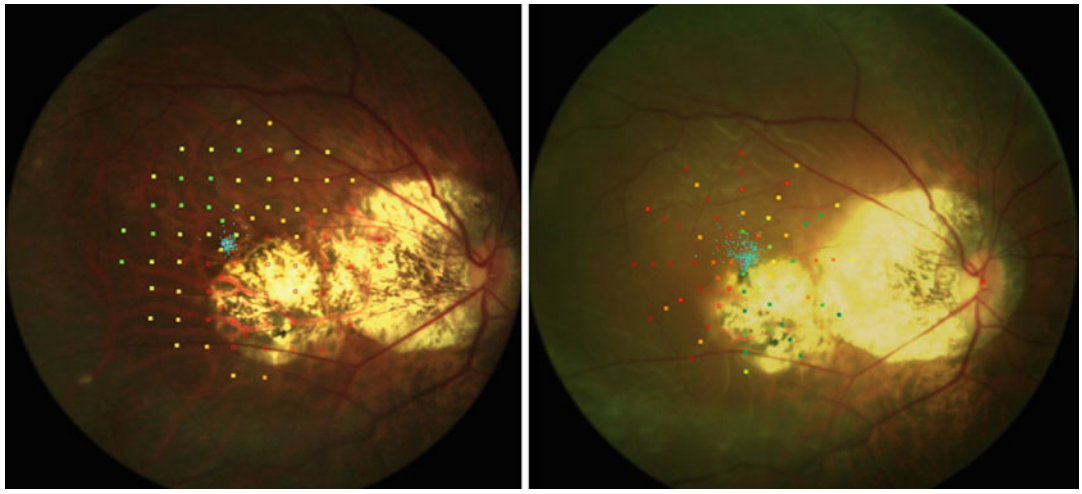

Fig. 13.3 Macular hole retinal detachment. A 70-year-old female with history of CNV removal surgery. Axial length is 29.57, and decimal visual acuity is 0.5 in the right eye (*left*). Large RPE atrophy is observed in the macular area and here a low sensitivity is measured (*right*). One year later, MHRD appears at the macula, and MP-1 shows a further sensitivity decrease

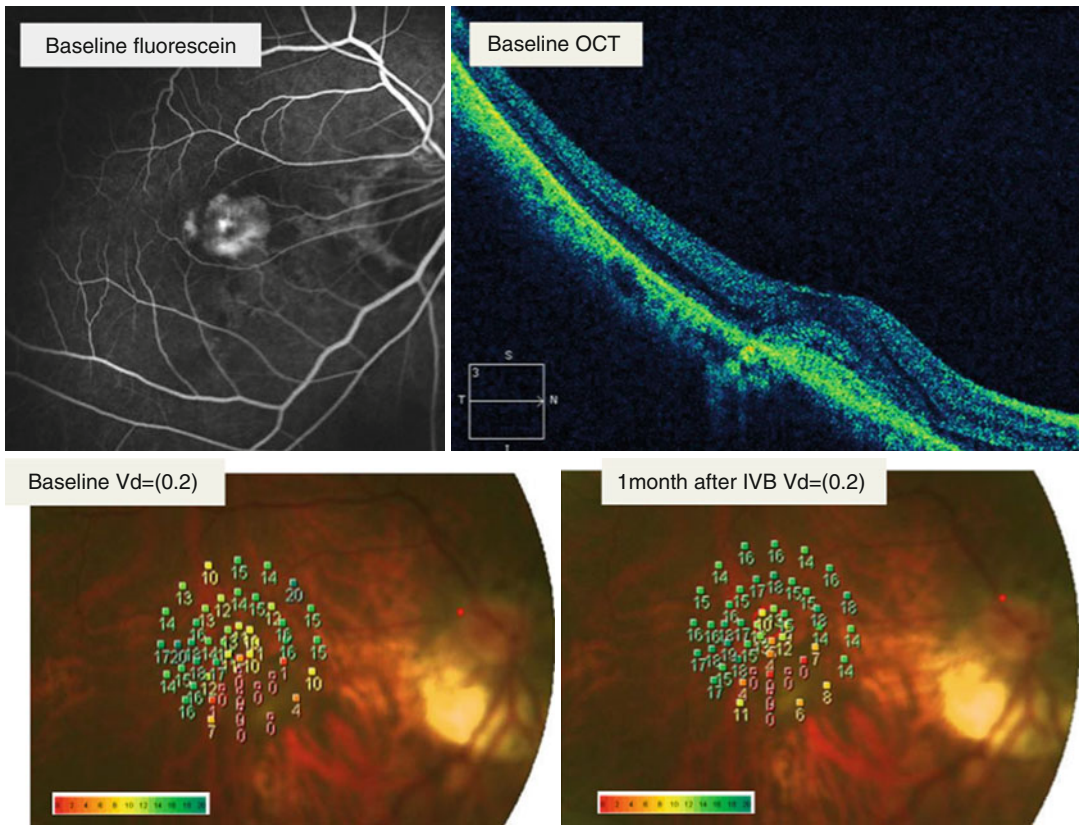

considered the most effective treatment for myopic CNV. Exudative lesions disappear for only a short time with intravitreal bevacizumab; however, a long-term follow-up still needs to be done.

Figure 13.4 refers to a case of a 72-year-old woman with myopic CNV in the right eye. Axial length of the right eye is 28.58 mm. Fluorescein angiography at the baseline shows a classic CNV lesion with early-phase leakage. OCT shows hyperreflective tissue above RPE representative characteristics of type 2 CNV. MP-1 shows the reduced sensitivity at the area corresponding to CNV. One month after intravitreal bevacizumab, visual acuity did not change at all; however, a slight improvement was measured on the MP-1.

Conclusions

Pathologic myopia often shows complications such as CNV, retinoshisis, foveal detachment, macular holes, and RPE atrophic changes. However, visual acuity is not enough a valuable index to evaluate the effectiveness of treatment or improvement in pathologic complicated myopia. Although we have several advanced devices, such as OCT, to evaluate morphological changes, we had not the possibility to measure functional changes. Now, in some cases MP-1 may provide helpful information about visual function more than visual acuity. The fixation training programs (reading test and feedback test) are also involved in MP-1 for patients with central scotoma. MP-1 is very helpful because it allows to use both research and clinical fields for pathologic myopia.

References

1. Wong WT, Brucker AJ (2005) Ocular findings in myopia. In: Midene E (ed) Myopia and related disease. Ophthalmic Communications Society Inc., New York, pp 54–65
2. Moriyama M, Ohno-Matsui K, Modegi T et al (2012) Quantitative analyses of high-resolution 3D MR images of highly myopic eyes to determine their shapes. Invest Ophthalmol Vis Sci 53:4510–4518
3. Moriyama M, Ohno-Matsui K, Hayashi K et al (2011) Topographic analyses of shape of eyes with pathologic myopia by high-resolution three-dimensional magnetic resonance imaging. Ophthalmology 118: 1626–1637
4. Scassa C, Ripandelli G, Sciamanna M et al (2005) The role of optical coherence tomography in the differential diagnosis of macular disease in high myopia. In: Midena E (ed) Myopia and related disease. Ophthalmic Communications Society Inc., New York, pp 90–93
5. Brancato R, Pierro L (2005) Optical coherence tomography findings in myopia. In: Midene E (ed) Myopia and related disease. Ophthalmic Communications Society Inc, New York, pp 87–89
6. Hee MR, Baumal CR, Puliafito C et al (1996) Optical coherence tomography of age-related macular degeneration and choroidal neovascularization. Ophthalmology 103:1260–1270
7. Phillips CI, Dobbie JG (1963) Posterior staphyloma and retinal detachment. Am J Ophthalmol 55:332–355
8. Ripandelli G, Parisi V, Friberg TR et al (2004) Retinal detachment associated with macular hole in high myopia: using the vitreous anatomy to optimize the surgical approach. Ophthalmology 111:726–731
9. Sayanagi K, Morimoto Y, Ikuno Y et al (2010) Spectral-domain optical coherence tomographic findings in myopic foveoschisis. Retina 30:623–628
10. Ikuno Y, Sayanagi K, Soga K et al (2008) Foveal anatomical status and surgical results in vitrectomy for myopic foveoschisis. Jpn J Ophthalmol 52:269–276
11. Hotchkiss ML, Fine SL (1981) Pathologic myopia and choroidal neovascularization. Am J Ophthalmol 91:1771–1783
12. Gaucher D, Erginay A, Lecleire-Collet A et al (2008) Dome-shaped macula in eyes with myopic posterior staphyloma. Am J Ophthalmol 145:909–914
13. Imamura Y, Iida T, Maruko I et al (2011) Enhanced depth imaging optical coherence tomography of the sclera in dome-shaped macula. Am J Ophthalmol 151:297–302
14. Maruko I, Iida T, Sugano Y et al (2011) Morphologic choroidal and scleral changes at the macula in tilted disc syndrome with staphyloma using optical coherence tomography. Invest Ophthalmol Vis Sci 52:8763–8768
15. Pilotto E (2006) Myopic maculopathy. In: Midene E (ed) Perimetry and the fundus: an introduction to microperimetry. Slack Inc., New Jersey, pp 109–115
16. Qin Y, Zhu M, Qu X et al (2010) Regional macular light sensitivity changes in myopic Chinese adults: an MP1 study. Invest Ophthalmol Vis Sci 51:4451–4457
17. Ripandelli G, Rossi T, Scarinci F et al (2012) Macular vitreoretinal interface abnormalities in highly myopic eyes with posterior staphyloma: 5-year follow-up. Retina 32:1531–1538
18. Gella L, Raman R, Sharma T et al (2011) Evaluation of in vivo human retinal morphology and function in myopes. Curr Eye Res 36:943–946
19. Scupola A, Tiberti AC, Sasso P et al (2010) Macular functional changes evaluated with MP-1 microperimetry after intravitreal bevacizumab for subfoveal myopic choroidal neovascularization: one-year results. Retina 30:739–747

20. Varano M, Tedeschi M, Oddone F et al (2010) Microperimetric retinal changes in myopic choroidal neovascularization treated with intravitreal ranibizumab. Retina 30:413–417
21. Yodoi Y, Tsujikawa A, Nakanishi H et al (2009) Central retinal sensitivity after intravitreal injection of bevacizumab for myopic choroidal neovascularization. Am J Ophthalmol 147:824, 824.e1
22. Varano M, Parisi V, Tedeschi M et al (2005) Macular function after PDT in myopic maculopathy: psychophysical and electrophysiological evaluation. Invest Ophthalmol Vis Sci 46:1453–1462
23. Ikuno Y, Sayanagi K, Ohji M et al (2004) Vitrectomy and internal limiting membrane peeling for myopic foveoschisis. Am J Ophthalmol 137: 719–724